

Structures, Metal–Ligand Bond Strength, and Bonding Analysis of Ferrocene Derivatives with Group-15 Heteroligands $\text{Fe}(\eta^5\text{-E}_5)_2$ and $\text{FeCp}(\eta^5\text{-E}_5)$ ($\text{E} = \text{N}, \text{P}, \text{As}, \text{Sb}$). A Theoretical Study[†]

Jan Frunzke, Matthias Lein, and Gernot Frenking*

Fachbereich Chemie, Philipps-Universität Marburg, Hans-Meerwein-Strasse, D-35032 Marburg, Germany

Received May 20, 2002

Quantum chemical DFT calculations using B3LYP and BP86 functionals have been carried out for the title compounds. The equilibrium geometries and bond dissociation energies are reported. The metal–ligand bonding was analyzed with an energy partitioning method. The strongest bonded homoleptic complex with a heterocyclic ligand is $\text{Fe}(\eta^5\text{-P}_5)_2$. The bond dissociation energy yielding the Fe atom and two *cyclo*-P₅ ligands ($D_0 = 128.3$ kcal/mol) is nearly the same as for ferrocene ($D_0 = 131.3$ kcal/mol). The nitrogen, arsenic, and antimony analogues of $\text{Fe}(\eta^5\text{-E}_5)_2$ have significantly weaker metal–ligand bonds, which, however, should still be strong enough to make them isolable under appropriate conditions. The calculated heats of formation show also that the phosphorus complex is the most stable species of the heterocyclic $\text{Fe}(\eta^5\text{-E}_5)_2$ series. The $\text{Fe}-(\eta^5\text{-E}_5)$ bonding in the mixed sandwich complexes $\text{FeCp}(\eta^5\text{-E}_5)$ is much stronger compared to the homoleptic molecules. The heterocyclic ligands *cyclo*-E₅ in the mixed complexes $\text{FeCp}(\eta^5\text{-E}_5)$ bind as strongly or in case of phosphorus even stronger than one Cp ligand does in FeCp_2 except for $\text{E} = \text{Sb}$. The metal fragments $\text{Fe}(\eta^5\text{-E}_5)^+$ have a pyramidal geometry except for $\text{E} = \text{Sb}$, which is predicted to be a planar ion with D_{5h} symmetry. The energy partitioning shows that the binding interactions between the closed shell *cyclo*-E₅[−] ligand and the $\text{Fe}(\eta^5\text{-E}_5)^+$ fragment do not change very much for the different ligand atoms E in the homoleptic and heteroleptic complexes. The bonding comes from 53%–58% electrostatic attraction, while 42%–47% come from covalent interactions. The latter contribution comes mainly from the donation of the occupied e_1 (π) orbital of the ligand into the empty orbital of the metal fragment.

1. Introduction

There is a ubiquitous number of transition metal (TM) complexes with cyclic conjugated ligands C_nH_n^q with $n = 3\text{--}8$ where the charge q can be positive, negative, or neutral.¹ The most important classes are those with $n = 5$ (metallocenes, sandwich and half-sandwich complexes) and $n = 6$ (arene complexes). The first example of the former system with the ligand C_5H_5^- (cyclopentadiene anion, Cp[−]) that could become synthesized was ferrocene FeCp_2 . The publication by Kealy and Pauson fifty years ago^{2,3} is considered a landmark event in organometallic chemistry.⁴ It opened a new field which became very important for synthetic^{1,5} and industrial⁶ applications. The initial suggestion of the structure

having two $\text{Fe}-\text{C}_5\text{H}_5$ σ -bonds² was corrected in two independent publications by Fischer and Pfab⁷ and by Wilkinson, Rosenblum, Whiting, and Woodward,⁸ who showed that the molecule has a π -bonded sandwich structure. It was soon recognized that one or more CH groups of the Cp ligand can be substituted by valence-isoelectronic group-15 elements $\text{E} = \text{N}, \text{P}, \text{As}, \text{Sb}$, yielding heterocyclopentadienyl ligands, which may also bind in an η^5 mode to a transition metal. Examples are the ligands pyrrolyl (NC_4H_4^-), pyrazolyl ($\text{N}_2\text{C}_3\text{H}_3^-$), phospholyl (PC_4H_4^-), arsoly (AsC_4H_4^-), 1,2,4-triphospholyl ($\text{P}_3\text{C}_2\text{H}_2^-$), and 1,2,4-stibadiphospholyl ($\text{SbP}_2\text{C}_2\text{H}_2^-$).⁹

The first synthesis of a complex with a heterocyclopentadiene ligand where all CH groups are substituted by a group-15 element was reported by Rheingold et al. in 1982.¹⁰ They synthesized the triple-decker complex $(\text{CpMo})_2(\mu, \eta^4\text{-As}_5)$, where the *cyclo*-As₅ ring is the bridg-

[†] Theoretical Studies of Inorganic Compounds, Part 20. Part 19: Loschen, C.; Voigt, K.; Frunzke, J.; Diefenbach, A.; Diedenhofen, M.; Frenking, G. *Z. Allg. Anorg. Chem.* **2002**, *628*, 1294.

* Corresponding author. E-mail: frenking@chemie.uni-marburg.de.

(1) (a) Abel, E. W.; Stone, F. G. A.; Wilkinson, G., Eds. *Comprehensive Organometallic Chemistry II*; Elsevier: Oxford, 1995. (b) Elschenbroich, Ch.; Salzer, A. *Organometallics*, 2nd ed.; VCH: Weinheim, 1992; p 309 f.

(2) Kealy, T. J.; Pauson, P. L. *Nature* **1951**, *168*, 1039.

(3) Another paper that reported on the synthesis of ferrocene was submitted earlier than ref 2, but it was published later: Miller, S. A.; Tebboth, J. A.; Tremaine, J. F. *J. Chem. Soc.* **1952**, 633.

(4) (a) Special issue of *J. Organomet. Chem.* **2001**, *637–639*. (b) Reference 1b, p 3.

(5) Togni, A.; Haltermann, R. L., Eds. *Metallocenes*; Wiley-VCH: New York, 1998.

(6) Cornils, B.; Herrmann, W. A., Eds. *Homogeneous Catalysis with Organometallic Compounds*; VCH: Weinheim, 1996; Vols. 1 and 2.

(7) Fischer, E. O.; Pfab, W. *Z. Naturforsch.* **1952**, *76*, 377.

(8) Wilkinson, G.; Rosenblum, M.; Whiting, M. C.; Woodward, R. B. *J. Am. Chem. Soc.* **1952**, *74*, 2125.

(9) (a) Nief, F. *Eur. J. Inorg. Chem.* **2001**, 891. (b) Reference 1b, p 376 f.

(10) Rheingold, A. L.; Foley, M. L.; Sullivan, P. J. *J. Am. Chem. Soc.* **1982**, *104*, 4727.

ing ligand between the CpMo moieties. The X-ray structure analysis of the complex shows large differences among the As–As distances, which led the authors to suggest that the *cyclo*-As₅ ligand binds in an η^4 -fashion and not η^5 .¹⁰ A complex with a truly η^5 -bonded *cyclo*-E₅ ligand was finally synthesized by Scherer et al. in 1986; they reported the synthesis and X-ray structure analysis of the triple-decker complex (Cp*Mo)₂(μ^5 -P₅) (Cp* = C₅Me₅).¹¹ One year later Scherer published also the synthesis of the pentaphosphaferrocene derivative Cp*Fe(η^5 -P₅).¹² The same author succeeded in 1990 in the synthesis of pentaarsaferrocene Cp*Fe(η^5 -As₅).¹³

The chemical bonding situation in ferrocene is usually discussed in terms of donor–acceptor interactions between Fe²⁺ (t_{2g}, d⁶) and two Cp⁻ ligands.¹⁴ The orbital interaction diagram of FeCp₂ having D_{5d} symmetry has contributions that arise from orbitals that have a_{1g}, a_{2u}, e_{1g}, e_{1u}, and e_{2g} symmetry. A recent energy partitioning analysis of the Fe²⁺(t_{2g}, d⁶)-(Cp⁻)₂ bonding using DFT calculations showed that the e_{1g} orbital interactions, which come from the (Cp⁻)₂→Fe²⁺ π -donation into the empty d(e_{1g}) orbitals of Fe contribute 65% of the total orbital interactions.¹⁵ It was also shown that 51% of the Fe²⁺(t_{2g}, d⁶)-(Cp⁻)₂ bonding is electrostatic and 49% is covalent. The same paper reported the theoretically predicted structure and bonding analysis of isoelectronic iron bispentazol Fe(η^5 -N₅)₂.¹⁵ The calculations showed that the strength of the binding interactions and the nature of the bonding between Fe²⁺ (t_{2g}, d⁶) and two Cp⁻ ligands are similar to the bonding between Fe²⁺ (t_{2g}, d⁶) and two *cyclo*-N₅⁻ ligands. Iron bispentazol was predicted to be thermodynamically much less stable than ferrocene because of the exothermic reaction Fe(η^5 -N₅)₂ → Fe + 5N₂ (-227 kcal/mol).¹⁵

It seems that the time is ripe for theoretical and experimental studies of homoleptic transition metal complexes with π -bonded heterocyclic ligands. Shortly after our theoretical paper about Fe(η^5 -N₅)₂ was published,¹⁵ a combined experimental/theoretical work reported the first synthesis of a carbon-free sandwich complex, Ti(η^5 -P₅)₂²⁻.¹⁶ It can be expected that more examples of the new class of compounds will soon become synthesized. It would be helpful if accurate theoretical calculations could predict which ligands would be the best candidates for stable complexes. At the same time it is desirable to learn about the nature of the bonding in the molecules.

The question that shall be addressed in this paper concerns the structures, stabilities, and bonding situations of the heavier analogues of iron bispentazole Fe-

(η^5 -E₅)₂ (E = P, As, Sb). To this end, we optimized the geometries and calculated the bond dissociation energies of the complexes using gradient-corrected density functional theory (DFT). We also calculated the “semisubstituted” species FeCp(η^5 -E₅) (E = N, P, As, Sb). The metal–ligand interactions were analyzed in a similar way as in our previous study¹⁵ about ferrocene and iron bispentazole using the energy partitioning scheme of the program ADF,¹⁷ which is based on the methods suggested by Morokuma¹⁸ and Ziegler.¹⁹ A short outline is given in the Methods section. The bonding situation and the stabilities of the pentaphospholyl complexes FeCp(η^5 -P₅) and Fe(η^5 -P₅)₂ have been the subject of previous theoretical studies at the EHT level.^{20,21} It was concluded that the CpFe-(η^5 -P₅) bonding in the former complex is rather strong,²⁰ while the orbital interactions in Fe(η^5 -P₅)₂ are much weaker than in ferrocene, and thus, it should be difficult to synthesize the compound.²¹ It will be interesting to compare the qualitative results of the EHT studies^{20,21} with the quantitative data given in the present work.

2. Methods

The geometries have been optimized first at the gradient-corrected DFT level using the three-parameter fit of the exchange–correlation potential suggested by Becke²² in conjunction with the LYP²³ exchange potential (B3LYP).²⁴ A nonrelativistic small-core ECP with a (441/2111/41) valence basis set for Fe²⁵ and 6-31G(d) basis sets²⁶ for C, N, H have been employed in the geometry optimizations. Relativistic ECPs with (211/211/1) valence basis sets were employed for the atoms P, As, and Sb.²⁷ This is our standard basis set II.²⁸ The nature of the stationary points was examined by calculating the Hessian matrix at B3LYP/II. The atomic partial charges have been estimated with the NBO method of Weinhold.²⁹ The calculations have been carried out with the program package Gaussian 98.³⁰

The iron–ligand bonding interactions in Fe(η^5 -E₅)₂ and FeCp(η^5 -E₅)₂ have been analyzed with the energy decomposition scheme of the program ADF.^{17,31} To this end, the geometries were optimized with the exchange functional of Becke³² and the correlation functional of Perdew³³ (BP86) in conjunction with uncontracted Slater-type orbitals (STOs) as basis functions.³⁴ Relativistic effects have been considered by the

(11) Scherer, O. J.; Schwalb, J.; Wolmershäuser, G.; Kaim, W.; Gross, R. *Angew. Chem.* **1986**, *98*, 346; *Angew. Chem., Int. Ed. Engl.* **1986**, *25*, 363.

(12) (a) Scherer, O. J.; Brück, T. *Angew. Chem.* **1987**, *99*, 59; *Angew. Chem., Int. Ed. Engl.* **1987**, *26*, 59. (b) Scherer, O. J.; Brück, T.; Wolmershäuser, G. *Chem. Ber.* **1988**, *121*, 935.

(13) Scherer, O. J.; Blath, C.; Wolmershäuser, G. *J. Organomet. Chem.* **1990**, *387*, C21.

(14) (a) Reference 1b, p 320. (b) Albright, T. A.; Burdett, J. K.; Whangbo, M. H. *Orbital Interactions in Chemistry*; Wiley: New York, 1985; p 393. (c) Cotton, F. A.; Wilkinson, G.; Murillo, C. A.; Bochmann, M. *Advanced Inorganic Chemistry*, 6th ed.; John Wiley: New York, 1999; p 686.

(15) Lein, M.; Frunzke, J.; Timoshkin, A.; Frenking, G. *Chem. Eur. J.* **2001**, *7*, 4155.

(16) Urnezisus, E.; Brennessel, W. W.; Cramer, C. J.; Ellis, J. E.; Schleyer, P. v. R. *Science* **2002**, *295*, 832.

(17) ADF99: (a) Barends, E. J.; Ellis, D. E.; Ros, P. *Chem. Phys.* **1973**, *2*, 41. (b) Versluis, L.; Ziegler, T. *J. Chem. Phys.* **1988**, *322*, 88. (c) te Velde, G.; Baerends, E. J. *J. Comput. Phys.* **1992**, *99*, 84. (d) Fonseca Guerra, C.; Snijders, J. G.; te Velde, G.; Barends, E. J. *Theor. Chim. Acta* **1998**, *99*, 391.

(18) Morokuma, K. *J. Chem. Phys.* **1971**, *55*, 1236.

(19) Ziegler, T.; Rauk, A. *Theor. Chim. Acta* **1977**, *46*, 1.

(20) Kerins, M. C.; Fitzpatrick, N. J.; Nguyen, M. T. *Polyhedron* **1989**, *8*, 1135.

(21) Chamizo, J. A.; Ruiz-Mazon, M.; Salcedo, R.; Toscano, R. A. *Inorg. Chem.* **1990**, *29*, 879.

(22) Becke, A. D. *J. Chem. Phys.* **1993**, *98*, 5648.

(23) Lee, C.; Yang, W.; Parr, R. G. *Phys. Rev. B* **1988**, *37*, 785.

(24) Stevens, P. J.; Devlin, F. J.; Chabrowski, C. F.; Frisch, M. J. *J. Phys. Chem.* **1994**, *98*, 11623.

(25) Hay, P. J.; Wadt, W. R. *J. Chem. Phys.* **1985**, *82*, 299.

(26) (a) Ditchfield, R.; Hehre, W. J.; Pople, J. A. *J. Chem. Phys.* **1971**, *54*, 724. (b) Hehre, W. J.; Ditchfield, R.; Pople, J. A. *J. Chem. Phys.* **1972**, *56*, 2257.

(27) Bergner, A.; Dolg, M.; Küchle, W.; Stoll, H.; Preuss, H. *Mol. Phys.* **1993**, *80*, 1431.

(28) Frenking, G.; Antes, I.; Böhme, M.; Dapprich, S.; Ehlers, A. W.; Jonas, V.; Neuhaus, A.; Otto, M.; Stegmann, R.; Veldkamp, A.; Vydroshchikov, S. F. In *Reviews in Computational Chemistry*; Lipkowitz, K. B., Boyd, D. B., Eds.; VCH: New York, 1996; Vol. 8, pp 63–144.

(29) Reed, A. E.; Curtiss, L. A.; Weinhold, F. *Chem. Rev.* **1988**, *88*, 899.

zero-order regular approximation (ZORA).³⁵ The basis set for Fe has triple- ζ quality augmented by one set of 6p functions. Triple- ζ basis sets augmented by two sets of d-type polarization functions have been used for the main group elements. The $(n-1)s^2$ and $(n-1)p^6$ core electrons of the main group elements and the $(1s2s2p)^{10}$ core electrons of Fe were treated by the frozen-core approximation.^{36a} An auxiliary set of s, p, d, f, and g STOs was used to fit the molecular densities and to represent the Coulomb and exchange potentials accurately in each SCF cycle.^{36b}

For the energy partitioning analysis the interaction energy ΔE_{int} was calculated and decomposed for the bonding between the metal fragments $\text{Fe}(\eta^5\text{-E}_5)^+$ and FeCp and the ligands $(\eta^5\text{-E}_5)^-$ in the 1A_1 and $^1A_1'$ ground state, respectively. The instantaneous interaction energy ΔE_{int} can be divided into three components:

$$\Delta E_{\text{int}} = \Delta E_{\text{elstat}} + \Delta E_{\text{Pauli}} + \Delta E_{\text{orb}} \quad (1)$$

ΔE_{elstat} gives the electrostatic interaction energy between the fragments which are calculated with a frozen electron density distribution in the geometry of the complex. It can be considered as an estimate of the *electrostatic* contribution to the bonding interactions. The second term in eq 1, ΔE_{Pauli} , gives the repulsive four-electron interactions between occupied orbitals. The last term gives the stabilizing orbital interactions, ΔE_{orb} , which can be considered as an estimate of the *covalent* contributions to the bonding. Thus, the ratio $\Delta E_{\text{elstat}}/\Delta E_{\text{orb}}$ indicates the electrostatic/covalent character of the bond. The latter term can be partitioned further into contributions by the orbitals that belong to different irreducible representations of the point group of the interacting system. This makes it possible to calculate, for example, the contributions of σ and π bonding to a covalent multiple bond.³⁷ Technical details about the ETS method can be found in the literature.³¹

The bond dissociation energy (BDE), ΔE_e , is given by the sum of ΔE_{int} and the fragment preparation energy ΔE_{prep} :

$$\Delta E_e = \Delta E_{\text{prep}} + \Delta E_{\text{int}} \quad (2)$$

(30) Frisch, M. J.; Trucks, G. W.; Schlegel, H. B.; Scuseria, G. E.; Robb, M. A.; Cheeseman, J. R.; Zakrzewski, V. G.; Montgomery, J. A.; Stratmann, R. E.; Burant, J. C.; Dapprich, S.; Milliam, J. M.; Daniels, A. D.; Kudin, K. N.; Strain, M. C.; Farkas, O.; Tomasi, J.; Barone, V.; Cossi, M.; Cammi, R.; Mennucci, B.; Pomelli, C.; Adamo, C.; Clifford, S.; Ochterski, J.; Petersson, G. A.; Ayala, P. Y.; Cui, Q.; Morokuma, K.; Malick, D. K.; Rabuck, A. D.; Raghavachari, K.; Foresman, J. B.; Cioslowski, J.; Ortiz, J. V.; Stefanov, B. B.; Liu, G.; Liashenko, A.; Piskorz, P.; Komaromi, I.; Gomberts, R.; Martin, R. L.; Fox, D. J.; Keith, T. A.; Al-Laham, M. A.; Peng, C. Y.; Nanayakkara, A.; Gonzalez, C.; Challacombe, M.; Gill, P. M. W.; Johnson, B. G.; Chen, W.; Wong, M. W.; Andres, J. L.; Head-Gordon, M.; Replogle, E. S.; Pople, J. A. *Gaussian 98* (Revision A.1); Gaussian Inc.: Pittsburgh, PA, 1998.

(31) (a) Bickelhaupt, F. M.; Baerends, E. J. *Rev. Comput. Chem.* Lipkowitz, K. B., Boyd, D. B., Eds.; Wiley-VCH: New York, 2000; Vol. 15, p 1. (b) te Velde, G.; Bickelhaupt, F. M.; Baerends, E. J.; van Gisbergen, S. J. A.; Fonseca Guerra, C.; Snijders, J. G.; Ziegler, T. J. *Comput. Chem.* **2001**, *22*, 931.

(32) Becke, A. D. *Phys. Rev. A* **1988**, *38*, 3098.

(33) Perdew, J. P. *Phys. Rev. B* **1986**, *33*, 8822.

(34) Snijders, J. G.; Baerends, E. J.; Vernooijs, P. *At. Nucl. Data Tables* **1982**, *26*, 483.

(35) (a) Chang, C.; Pelissier, M.; Durand, Ph. *Phys. Scr.* **1986**, *34*, 394. (b) Heully, J.-L.; Lindgren, I.; Lindroth, E.; Lundquist, S.; Martensson-Pendrill, A.-M. *J. Phys. B* **1986**, *19*, 2799. (c) van Lenthe, E.; Baerends, E. J.; Snijders, J. G. *J. Chem. Phys.* **1993**, *99*, 4597. (d) van Lenthe, E.; Baerends, E. J.; Snijders, J. G. *J. Chem. Phys.* **1996**, *105*, 6505. (e) van Lenthe, E.; van Leeuwen, R.; Baerends, E. J.; Snijders, J. G. *Int. J. Quantum Chem.* **1996**, *57*, 281.

(36) (a) Baerends, E. J.; Ellis, D. E.; Ros, P. *Chem. Phys.* **1973**, *2*, 41. (b) Krijn, J.; Baerends, E. J. *Fit Functions in the HFS-Method*; Internal Report (in Dutch), Vrije Universiteit Amsterdam: The Netherlands, 1984.

(37) (a) Diefenbach, A.; Bickelhaupt, F. M. *J. Am. Chem. Soc.* **2000**, *122*, 6449. (b) Uddin, J.; Frenking, G. *J. Am. Chem. Soc.* **2001**, *123*, 1683. (c) Chen, Y.; Frenking, G. *J. Chem. Soc., Dalton Trans.* **2001**, 434.

ΔE_{prep} is the energy that is necessary to promote the fragments from their equilibrium geometry and electronic ground state to the geometry and electronic state that they have in the optimized structure.

3. Geometries and Bond Dissociation Energies

Table 1 shows the most important bond lengths and energy values of the homoleptic complexes $\text{Fe}(\eta^5\text{-E}_5)_2$ and some fragments. Figure 1 displays the optimized geometries of $\text{Fe}(\eta^5\text{-P}_5)_2$ and the phosphorus-containing fragments. The structures of the other molecules except $\text{Fe}(\eta^5\text{-Sb}_5)^+$ are very similar, and therefore, they are not shown. The geometry optimization of $\text{Fe}(\eta^5\text{-Sb}_5)^+$ yielded a planar structure (Figure 1), while the other $\text{Fe}(\eta^5\text{-E}_5)^+$ cations are predicted with a pyramidal geometry. The full geometries and total energies are given as Supporting Information.

The geometry optimizations of $\text{Fe}(\eta^5\text{-E}_5)_2$ have been carried out with D_{5h} and D_{5d} symmetry. The B3LYP/II calculations predict that the cyclic ligands in $\text{Fe}(\eta^5\text{-N}_5)_2$ and $\text{Fe}(\eta^5\text{-Sb}_5)_2$ have a staggered conformation (D_{5d} symmetry), while the complexes $\text{Fe}(\eta^5\text{-Cp})_2$, $\text{Fe}(\eta^5\text{-P}_5)_2$, and $\text{Fe}(\eta^5\text{-As}_5)_2$ have eclipsed ligands (D_{5h} symmetry). The energy differences between the D_{5d} and D_{5h} conformations are very low, however. The calculations predict that the barriers for ring rotation are ≤ 2.6 kcal/mol, the highest value being calculated for $\text{Fe}(\eta^5\text{-Sb}_5)_2$. The BP86/TZ2P calculations give very similar values for the bond lengths and for the D_{5d} - D_{5h} energy differences. The D_{5d} form of $\text{Fe}(\eta^5\text{-As}_5)_2$ is predicted, however, to be slightly (-0.1 kcal/mol) lower in energy than the D_{5h} form. The B3LYP/II optimization of the D_{5d} form of $\text{Fe}(\eta^5\text{-As}_5)_2$ failed because of convergence problems. The calculation of the vibrational frequencies of the D_{5h} form showed that it is an energy minimum at this level of theory. The calculated geometry of ferrocene is in good agreement with a gas-phase measurement, which shows that the molecule has indeed D_{5h} symmetry.³⁸ The X-ray structure analysis of $\text{Ti}(\eta^5\text{-P}_5)_2^{2-}$ showed that the P_5 rings are eclipsed like in the calculated geometry of $\text{Fe}(\eta^5\text{-P}_5)_2$.¹⁶

The metal fragments $\text{Fe}(\eta^5\text{-E}_5)^+$ have a pyramidal geometry and a singlet (1A_1) electronic ground state (C_{5v} symmetry) except for E = Sb. The geometry optimization of $\text{Fe}(\eta^5\text{-Sb}_5)^+$ at both levels of theory yielded a planar structure (D_{5h}), which has a ($^1A_1'$) singlet ground state. The calculated Fe-Sb bond length of $\text{Fe}(\eta^5\text{-Sb}_5)^+$ is very short (2.491 Å at B3LYP/II; 2.522 Å at BP86/TZ2P), which is nearly 0.5 Å shorter than in $\text{Fe}(\eta^5\text{-Sb}_5)_2$ (Table 1). The Fe-E distances of the other cations $\text{Fe}(\eta^5\text{-E}_5)^+$ are also shorter than in the neutral molecules $\text{Fe}(\eta^5\text{-E}_5)_2$, but the shortening is not so dramatic. The structure and bonding of $\text{Fe}(\eta^5\text{-Sb}_5)^+$ and related planar species will be the subject of a future study.³⁹

The neutral ligands *cyclo*-E₅ with a planar geometry are Jahn-Teller systems. Cp and *cyclo*-N₅ have nearly degenerate 2A_1 and 2B_1 doublet states (C_{2v} symmetry).

(38) Haaland, A.; Nilsson, J. E. *Acta Chem. Scand.* **1968**, *22*, 2653.

(39) Lein, M.; Frunzke, J.; Frenking, G. To be published.

(40) Freyberg, D. P.; Robbins, J. L.; Raymond, K. N.; Smart, J. C. *J. Am. Chem. Soc.* **1979**, *101*, 892.

(41) (a) Diedenhofen, M.; Wagener, T.; Frenking, G. In *Computational Organometallic Chemistry*; Cundari, T. R., Ed.; Marcel Dekker: New York, 2001; pp 69-121. (b) Jonas, V.; Frenking, G.; Reetz, M. T. *J. Am. Chem. Soc.* **1994**, *116*, 8741.

Table 1. Calculated Bond Lengths (Å) and Energies (kcal/mol) of Fe(E₅)₂ Complexes and Some Fragments at B3LYP/II (calculated values at BP86/TZ2P are given in parentheses)

molecule	symmetry	state	Fe–E	Fe–X ^a	E–E	i ^b	E _{rel}	D _e ^c	D ₀ ^{c,d}
Fe(Cp) ₂	D _{5h}	¹ A ₁ '	2.072 (2.059)	1.678 (1.658)	1.428 (1.435)	0	0.0	139.4	131.3
Fe(Cp) ₂	D _{5d}	¹ A _{1g}	2.074 (2.062)	1.682 (1.663)	1.428 (1.434)	1	0.7 (1.1)		
Fe(N ₅) ₂	D _{5h}	¹ A ₁ '	2.055 (2.011)	1.700 (1.636)	1.357 (1.375)	1	0.0		
Fe(N ₅) ₂	D _{5d}	¹ A _{1g}	2.054 (2.019)	1.699 (1.647)	1.357 (1.373)	0	–0.2 (–0.1)	107.0	97.1
Fe(P ₅) ₂	D _{5h}	¹ A ₁ '	2.505 (2.490)	1.705 (1.688)	2.158 (2.153)	0	0.0	131.9	128.3
Fe(P ₅) ₂	D _{5d}	¹ A _{1g}	2.507 (2.513)	1.707 (1.726)	2.158 (2.148)	1	0.7 (3.5)		
Fe(As ₅) ₂	D _{5h}	¹ A ₁ '	2.655 (2.671)	1.754 (1.722)	2.345 (2.401)	0	0.0	93.6	112.8?
Fe(As ₅) ₂	D _{5d}	¹ A _{1g}	^e (2.657)	^e (1.697)	^e (2.404)		–0.1 0.0		
Fe(Sb ₅) ₂	D _{5h}	¹ A ₁ '	2.977 (2.979)	1.883 (1.792)	2.717 (2.798)	1	0.0		
Fe(Sb ₅) ₂	D _{5d}	¹ A _{1g}	2.955 (2.979)	1.840 (1.787)	2.710 (2.802)	0	–2.6 (–4.1)	80.0	78.5
Fe(Cp) ⁺	C _{5v}	¹ A ₁	2.037 (1.997)	1.633 (1.578)	1.431 (1.439)	0			
Fe(N ₅) ⁺	C _{5v}	¹ A ₁	^e (1.885)	^e (1.458)	^e (1.404)				
Fe(P ₅) ⁺	C _{5v}	¹ A ₁	2.280 (2.233)	1.323 (1.242)	2.184 (2.182)	0			
Fe(As ₅) ⁺	C _{5v}	¹ A ₁	2.388 (2.357)	1.260 (1.084)	2.385 (2.461)	0			
Fe(Sb ₅) ⁺	D _{5h}	¹ A ₁ '	2.491 (2.522)	0.000 (0.000)	2.929 (2.968)	0			
Cp	C _{2v}	² A ₁			1.438; 1.371; 1.483	0			
<i>cyclo</i> -N ₅	C _{2v}	² A ₁			1.376; 1.239; 1.516	0			
<i>cyclo</i> -P ₅	C _{2v}	² A ₁			2.192; 2.115; 2.145	1	0.0		
<i>cyclo</i> -P ₅	C ₁	² A			2.096; 2.224; 2.117; 2.146; 2.196	0	–0.8		
<i>cyclo</i> -As ₅	C _{2v}	² A ₁			2.305; 2.385; 2.338	1	0.0		
<i>cyclo</i> -As ₅	C _s	² A			2.448; 2.292; 2.381	0	–2.3		
<i>cyclo</i> -Sb ₅	C _{2v}	² B ₁			2.687; 2.754; 2.702	1	0.0		
<i>cyclo</i> -Sb ₅	C _s	² A			2.843; 2.682; 2.773	0	–4.4		
<i>cyclo</i> -N ₅ [–]	D _{5h}	¹ A ₁ '			1.330 (1.335)	0			
<i>cyclo</i> -P ₅ [–]	D _{5h}	¹ A ₁ '			2.146 (2.143)	0			
<i>cyclo</i> -As ₅ [–]	D _{5h}	¹ A ₁ '			2.337 (2.399)	0			
<i>cyclo</i> -Sb ₅ [–]	D _{5h}	¹ A ₁ '			2.723 (2.795)	0			

^a X is the midpoint of the E₅ ring. ^b Number of imaginary frequencies. ^c Dissociation energies for the reaction Fe(E₅)₂ → Fe + 2E₅. ^d Includes ZPE corrections. ^e The calculation at B3LYP/II did not converge.

The former electronic state is slightly (<0.1 kcal/mol) lower in energy than the latter. The heavy-atom ligands *cyclo*-E₅ have nonplanar equilibrium geometries with C₁ symmetry (E = P) or C_s symmetry (E = As, Sb).⁴⁶ The electronic ground state of the aromatic anions *cyclo*-E₅[–] is ¹A₁'.

Table 2 shows the calculated bond lengths of the complexes FeCp(η⁵-E₅). The equilibrium structures have the Cp and *cyclo*-E₅ ligands in an eclipsed position (C_{5v} symmetry), but the staggered conformations (C_s symmetry) are only <1 kcal/mol higher in energy. The latter

(42) Ryan, M. F.; Eyler, J. R.; Richardson, D. E. *J. Am. Chem. Soc.* **1992**, *114*, 8611.

(43) Lias, S. G.; Bartmess, J. E.; Liebman, J. F.; Holmes, J. L.; Levin, R. D.; Mallard, W. G. *J. Phys. Chem. Ref. Data* **1988**, *17*, Suppl. 1.

(44) The experimental values were taken from ref 43: ΔH_f^o(Fe) = 99 kcal/mol; ΔH_f^o(C₂H₂) = 54.7 kcal/mol; ΔH_f^o(P₂) = 34.4 kcal/mol; ΔH_f^o(As₂) = 53.1 kcal/mol; ΔH_f^o(Sb₂) = 56.3 kcal/mol; ΔH_f^o(Cp) = 58.1 kcal/mol; ΔH_f^o(FeCp₂) = 58.0 kcal/mol.

(45) Reference 14b, p 388 f.

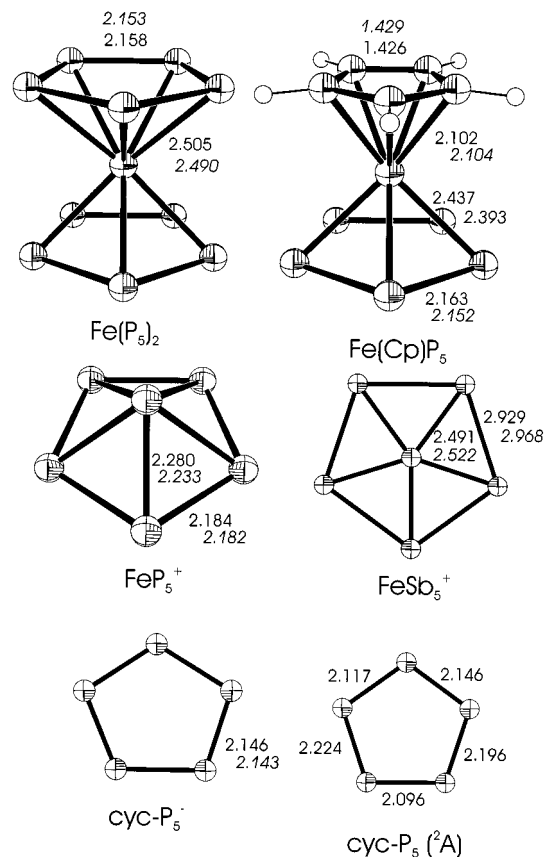


Figure 1. Calculated geometries of the phosphorus-containing molecules and $\text{Fe}(\eta^5\text{-Sb}_5)^+$ at B3LYP/II. The BP86/TZ2P data are given in *italics*. All values in Å.

conformations have not been calculated at BP86/TZ2P because the results for the homoleptic complexes at the two levels of theory were very similar to each other. The comparison of the calculated bond lengths of $\text{FeCp}(\eta^5\text{-E}_5)$ with $\text{Fe}(\eta^5\text{-E}_5)_2$ shows that the Fe–C distances become longer and the Fe–E bond lengths become shorter in the former compounds except for E = N. The finding suggests that the Cp ligand in $\text{FeCp}(\eta^5\text{-E}_5)$ enhances the Fe–($\eta^5\text{-E}_5$) bonding for E = P, As, Sb, but it weakens the Fe–($\eta^5\text{-N}_5$) bonding compared with the homoleptic complexes $\text{Fe}(\eta^5\text{-E}_5)_2$. The bonding analysis that is presented below shows that this is indeed the case.

The theoretically predicted geometries of $\text{FeCp}(\eta^5\text{-P}_5)$ and $\text{FeCp}(\eta^5\text{-As}_5)$, which are shown in Figure 1, can be compared with the experimental structures of the related complexes $\text{FeCp}^*(\eta^5\text{-P}_5)$ and $\text{FeCp}^{**}(\eta^5\text{-As}_5)$ ($\text{Cp}^* = \text{C}_5\text{Me}_4\text{Et}$), which have been determined by X-ray structure analysis.^{12b,13} The experimental structures have the Cp^* and *cyclo*-E₅ (E = P, As) ligands in a staggered conformation. This is probably caused by the alkyl substituents of the Cp^* ring. The experimental geometry of $\text{Fe}(\text{Cp}^*)_2$ also has a staggered conformation,⁴⁰ while FeCp_2 has an eclipsed conformation.³⁸ We want to point out that the measured Fe–C distances of

$\text{FeCp}^*(\eta^5\text{-P}_5)$ and $\text{FeCp}^*(\eta^5\text{-As}_5)$ are ~ 0.04 Å longer than in $\text{Fe}(\text{Cp}^*)_2$.^{12b,13} This is in perfect agreement with the calculated distances of $\text{FeCp}(\eta^5\text{-P}_5)$, $\text{FeCp}(\eta^5\text{-As}_5)$, and FeCp_2 , which show (Tables 1, 2) that the Fe–C bond length of the latter complex is ~ 0.04 Å shorter than in the former two species. The absolute values of the calculated Fe–P and Fe–As bond lengths in $\text{FeCp}(\eta^5\text{-P}_5)$ and $\text{FeCp}(\eta^5\text{-As}_5)$ are ~ 0.08 Å longer than the experimental data. Three factors may explain the difference between theory and experiment: (i) Cp^* may enhance the Fe–($\eta^5\text{-P}_5$) and Fe–($\eta^5\text{-As}_5$) bonding in the experimental structures more than Cp does in the calculated species; (ii) solid state effects which always tend to shorten metal–ligand bonds;⁴¹ (iii) error in the theoretical method. It is difficult to decide which factors are mainly responsible for the different values.

We calculated the energies of metal–ligand dissociation reactions in order to estimate the strength of the Fe–($\eta^5\text{-E}_5$) binding interactions. The results are shown in Table 3. Reactions 1–5 in Table 3 refer to the homoleptic complexes, and reactions 6–13 refer to the heteroleptic complexes. The energy values in the discussion come from B3LYP/II calculations unless otherwise noted.

Reaction 1 gives the total bonding energy of the *cyclo*-E₅ ligands with the iron atom in its ($4s^23d^6$) ⁵D ground state. Experimental values are available for ferrocene, which may be used in order to estimate the accuracy of the theoretical results. The calculated value for the bond dissociation energy of ferrocene including ZPE corrections (131.3 kcal/mol) is lower than the measured value (158 ± 2 kcal/mol).⁴² The theoretical result for the heterolytic bond cleavage of FeCp_2 yielding 2 Cp[−] and Fe²⁺ in its ($4s^23d^4$) ⁵D ground state (645.7 kcal/mol, reaction 2) is ~ 10 kcal/mol higher than the measured value, but it is within the experimental error range (635 ± 15 kcal/mol).⁴² The third reaction of ferrocene for which an experimental value is available is reaction 5. The measured heats of formation of FeCp_2 (58 kcal/mol), acetylene (54.7 kcal/mol), and Fe (99 kcal/mol) give for the dissociation of ferrocene into acetylene and Fe atom an experimental value of 314.5 kcal/mol.⁴³ The calculated value (302.6 kcal/mol) is 11.9 kcal/mol too low. We want to emphasize, however, that the aim of the energy calculations is to establish the trend of the bond energies, which we expect to be reliable.

Table 3 shows (reaction 1) that the calculated metal–ligand binding energy of iron bispentazole $\text{Fe}(\eta^5\text{-N}_5)_2$ (−107.0 kcal/mol) is 32 kcal/mol less than for ferrocene (−139.4 kcal/mol). Thus, the average Fe–($\eta^5\text{-E}_5$)₂ bond strength for one pentazole ligand is 16 kcal/mol lower than for one Cp ligand. The calculated values of reaction 1 indicate that the Fe–($\eta^5\text{-E}_5$)₂ binding energy increases significantly from nitrogen (−107.0 kcal/mol) to phosphorus (−131.9 kcal/mol), but then it decreases strongly for arsenic (−93.6 kcal/mol) and antimony (−80.0 kcal/mol). The theoretically predicted Fe–($\eta^5\text{-E}_5$) bond energies of reaction 1 thus suggest that the phosphorus complex is the strongest bonded π -heterocyclic complex of the $\text{Fe}(\eta^5\text{-E}_5)_2$ species, which is nearly as strongly bonded as ferrocene, while the antimony complex has the weakest bond. The reaction energies of the heterolytic bond cleavage (reaction 2) show also that the phosphorus complex has the highest Fe^{2+} –($\eta^5\text{-E}_5$)^{−2}

(46) Previous theoretical studies reported that the lowest lying form of P_5 ^{46a} has C_s symmetry and that the most stable form of As_5 ^{46b} has C_{2v} symmetry. Our calculations suggest that the C_1 form of P_5 and the C_s form of As are the global energy minima on the PES. (a) Chen, M. D.; Huang, R. B.; Zheng, L. S.; Zhang, Q. E.; Au, C. T. *Chem. Phys. Lett.* **2000**, *325*, 22. (b) Ballone, P.; Jones, R. O. *J. Chem. Phys.* **1994**, *100*, 4941.

Table 2. Calculated Bond Lengths (Å) and Energies (kcal/mol) of FeCp(E₅) at B3LYP/II (calculated values at BP86/TZ2P are given in parentheses)

molecule	symm.	state	Fe–C	Fe–E	Fe–X _{Cp} ^a	Fe–X _{E5} ^b	E–E	C–C	i ^c	E _{rel}	D _e ^d	D ₀ ^{d,e}
FeCp(N ₅)	C _{5v}	¹ A ₁	2.055 (2.056)	2.072 (2.021)	1.658 (1.657)	1.720 (1.648)	1.357 (1.376)	1.427 (1.431)	0	0.0	137.8	129.2
FeCp(N ₅)	C _s	¹ A	2.056	2.075	1.659	1.723	1.357	1.427	1	0.2		
FeCp(P ₅)	C _{5v}	¹ A ₁	2.102 (2.104)	2.437 (2.393)	1.716 (1.717)	1.599 (1.542)	2.163 (2.152)	1.426 (1.429)	0	0.0	146.2	139.9
FeCp(P ₅)	C _s	¹ A	2.107	2.438	1.722	1.598	2.163	1.425	1	0.7		
FeCp(As ₅)	C _{5v}	¹ A ₁	2.098 (2.093)	2.575 (2.578)	1.712 (1.704)	1.622 (1.568)	2.349 (2.406)	1.426 (1.429)	0	0.0	137.0	131.1
FeCp(As ₅)	C _s	¹ A	2.104	2.575	1.719	1.623	2.348	1.425	1	0.8		
FeCp(Sb ₅)	C _{5v}	¹ A ₁	2.099 (2.089)	2.849 (2.847)	1.714 (1.699)	1.665 (1.571)	2.718 (2.792)	1.426 (1.429)	0	0.0	119.8	114.4
FeCp(Sb ₅)	C _s	¹ A	2.107	2.849	1.723	1.666	2.717	1.425	1	0.7		

^a X is the midpoint of the Cp ring. ^b X is the midpoint of the E₅ ring. ^c Number of imaginary frequencies. ^d Dissociation energies for the reaction FeCp(E₅) → Fe + Cp + E₅. ^e Includes ZPE corrections.

Table 3. Calculated Reaction Energies and Heats of Formation ΔH_f^o (kcal/mol) at B3LYP/II (ZPE corrected values are given in parentheses; values at BP86/TZ2P are given in *italics*)

	CH	N	P	As	Sb
1 ^d Fe + 2 E ₅ → Fe(E ₅) ₂	-139.4 (-131.3)	-107.0 (-97.1)	-131.9 (-128.3)	-93.6 (-112.8)	-80.0 (-78.5)
2 ^e Fe ²⁺ + 2 E ₅ ⁻ → Fe(E ₅) ₂	-653.9 (-645.7)	-459.9 (-459.2)	-524.9 (-522.7)	-502.0 (-499.9)	-497.9 (-497.0)
3 ^e Fe ²⁺ + E ₅ ⁻ → Fe(E ₅) ⁺	-412.6 (-408.9)	<i>c</i>	-355.7 (-356.4)	-360.9 (-360.1)	-378.0 (-377.3)
4 Fe(E ₅) ⁺ + E ₅ ⁻ → Fe(E ₅) ₂	-241.3 (-236.9)	<i>c</i>	-169.2 (-166.4)	-141.1 (-139.8)	-119.9 (-119.6)
5 ^d Fe + 5 E ₂ → Fe(E ₅) ₂	-325.2 (-302.6)	201.4 (211.8)	-171.5 (-170.7)	-160.5 (-160.2)	-118.8 (118.7)
ΔH _f ^o (Fe(E ₅) ₂) ^a	69.9	310.8	108.3	222.7	227.0
6 ^d Fe + Cp + E ₅ → Fe(Cp)E ₅	-139.4 (-130.4)	-137.8 (-129.2)	-146.2 (-139.9)	-137.0 (-131.1)	-119.8 (-114.4)
7 Fe(Cp)E ₅ + Cp → FeCp ₂ + E ₅	0.0	-0.6 (-1.2)	7.8 (9.5)	-1.5 (0.8)	-18.6 (-16.0)
8 Fe(Cp)E ₅ + E ₅ → Fe(E ₅) ₂ + Cp	0.0	30.8 (30.4)	14.3 (11.6)	21.6 (18.3)	39.7 (35.9)
9 2 Fe(Cp)E ₅ → Fe(E ₅) ₂ + FeCp ₂	0.0	-29.2 (-30.0)	-21.1 (-20.2)	-41.0 (-40.1)	-20.2 (-19.0)
10 ^e Fe ²⁺ + Cp ⁻ + E ₅ ⁻ → Fe(Cp)E ₅	-653.9 (-645.7)	-571.7 (-567.0)	-600.2 (-594.8)	-598.6 (-593.5)	-586.2 (-581.3)
11 Fe(E ₅) ⁺ + Cp ⁻ → Fe(Cp)E ₅	-241.3 (-236.9)	<i>c</i>	-244.5 (238.4)	-237.7 (-233.4)	-208.2 (-204.0)
	-234.8 (231.3)	-288.7 (-283.7)	-220.4 (-216.4)	-213.6 (-209.8)	-190.7 (187.1)
12 FeCp ⁺ + E ₅ ⁻ → Fe(Cp)E ₅	-241.3 (-236.9)	-159.6 (-158.2)	-188.0 (-185.9)	-186.5 (-184.6)	-174.1 (-172.4)
	-234.8 (231.3)	-158.4 (-157.8)	-209.4 (-207.6)	-197.9 (-196.6)	-182.2 (-181.1)
13 2 FeCp ₂ + 5 E ₂ → 2 FeCp(E ₅) + 2 Cp	-186.8 (-172.2)	309.7 (313.0)	-52.5 (-53.4)	-49.7 (-52.8)	-38.7 (-43.1)
ΔH _f ^o (Fe(Cp)E ₅) ^b	50.6	156.4	59.2	106.3	119.1

^a Calculated from the energies of reaction 5 including ZPE corrections using the experimental heats of formation of Fe and E₂.⁴⁴

^b Calculated from the energies of reaction 12 including ZPE corrections using the experimental heats of formation of FeCp₂, E₂, and Cp.⁴⁴

^c The calculation of Fe(N₅)⁺ at B3LYP/II did not converge. ^d The Fe atom was calculated in the (3d⁶4s²) ⁵D electronic ground state. ^e The Fe²⁺ ion was calculated in the (3d⁶) ⁵D electronic ground state.

binding energy of the π-heterocyclic molecules, while the nitrogen complex has the lowest binding energy. Reactions 3 and 4 give the reaction energies of the stepwise addition of *cyclo*-E₅⁻ to Fe²⁺. The addition of the first ligand anion is more exothermic than the second, which is not surprising.

The calculated energies of reaction 5 are very interesting because they can be used to predict the heats of formation of the complexes using the experimentally known ΔH_f^o values of Fe and E₂.^{43,44} The theoretical value of ferrocene ΔH_f^o = 69.9 kcal/mol is in reasonable agreement with the experimental value 58 ± 0.7 kcal/mol. The highest value is calculated for iron bispentazole, which is a truly energy rich species (ΔH_f^o = 310.8 kcal/mol). The phosphorus complex has clearly the lowest heat of formation among the heteroferrocenes. The theoretical value of Fe(η⁵-P₅)₂ (ΔH_f^o = 108.3 kcal/mol) is only ~40 kcal/mol higher than that of ferrocene, but it is more than 100 kcal/mol lower than the heats of formation of Fe(η⁵-Sb₅)₂ (ΔH_f^o = 222.7 kcal/mol) and Fe(η⁵-As₅)₂ (ΔH_f^o = 227.0 kcal/mol).

Reactions 6–13 of Table 3 pertain to the mixed complexes FeCp(η⁵-E₅). It is interesting to note that the pentazole ligand in FeCp(η⁵-N₅) is nearly as strongly bonded as one Cp ligand in ferrocene. The total binding energy of Cp and *cyclo*-N₅ in FeCp(η⁵-N₅) (137.8 kcal/

mol, reaction 6) is similar to the total binding energy in ferrocene (139.4 kcal/mol), and thus, the ligand exchange reaction 7 of the two complexes is nearly thermoneutral. The pentaphospholyl ligand in FeCp(η⁵-P₅) is even 7.8 kcal/mol stronger bonded than one Cp ligand in ferrocene. It is the only heterocyclic species *cyclo*-E₅ for which the ligand exchange reaction of FeCp(η⁵-E₅) with Cp yielding ferrocene is endoenergetic (reaction 7). It shows that the phosphorus complex FeCp(η⁵-E₅) is the strongest bonded species of the mixed compounds FeCp(η⁵-E₅). Substitution of Cp by *cyclo*-E₅ in the latter species yielding Fe(η⁵-E₅)₂ is endothermic (reaction 8), but the least endothermic reaction is for E = P. The disproportionation reaction of the mixed complexes FeCp(η⁵-E₅) yielding the homoleptic species FeCp₂ and Fe(η⁵-E₅)₂ (reaction 9) shows directly the bond-strengthening effect of the Cp ligand upon the Fe–(η⁵-E₅) binding in the heterolytic compounds compared to the homoleptic complexes. The reactions are clearly exoenergetic. The most exoenergetic reaction is found for FeCp(η⁵-As₅) because the binding energy in FeCp(η⁵-As₅) is nearly as high as in the carbon and nitrogen analogues, but the binding energy of Fe(η⁵-As₅)₂ is very low.

The calculated energies of the heterolytic bond cleavage reactions 10–12 reveal also that the phosphorus

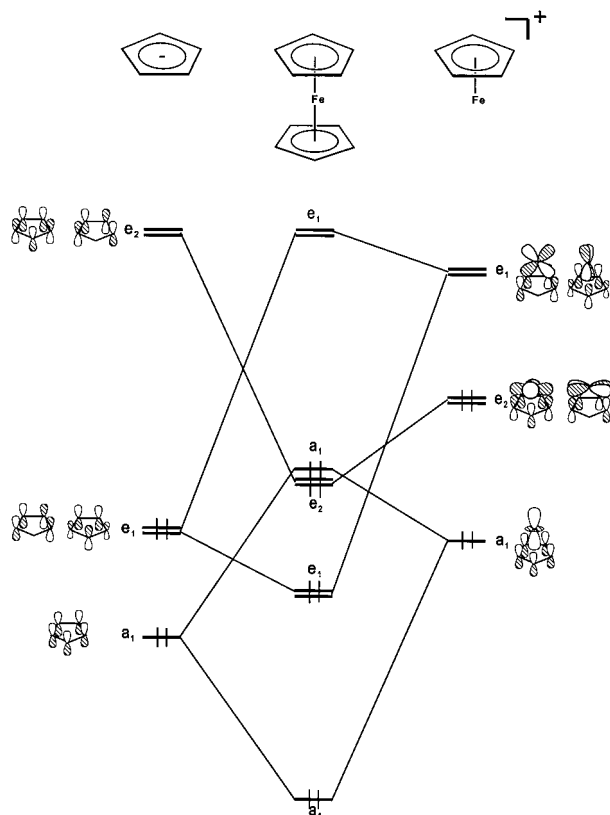


Figure 2. Orbital correlation diagram showing the most important orbitals of the ligand $cyclo-E_5^-$ and the fragment $Fe(\eta^5-E_5)^+$, which are relevant for the bonding in $Fe(\eta^5-E_5)_2$.

ring is the strongest bonded ligand, although the difference from the arsenic ligand is not very large. Reaction 13 has been included in Table 3 because it can be used to predict the heats of formation of the mixed complexes $FeCp(\eta^5-E_5)$. The calculated ΔH_f° values support the previous conclusion that the phosphorus species is the thermodynamically most stable $FeCp(\eta^5-E_5)$ molecule. The heats of formation of the latter species with heteroligands $cyclo-E_5$ are about half the values of the homoleptic complexes $Fe(\eta^5-E_5)_2$. We also want to point out that the bonding energy of one $cyclo-E_5^-$ ligand in the homoleptic complexes $Fe(\eta^5-E_5)_2$ is lower than in $FeCp(\eta^5-E_5)$ when $E = P, As, Sb$ but not for $E = N$ (compare reactions 4 and 12). This means that the Cp ligand weakens the iron–nitrogen bonding in $FeCp(\eta^5-N_5)$ compared with $Fe(\eta^5-N_5)_2$, but it enhances the bonding interactions of Fe with the heavier $cyclo-E_5$ in the heteroleptic sandwich complexes. This is in agreement with the calculated bond lengths which were discussed above.

4. Bonding Analysis

In our previous theoretical study on the bonding situation in ferrocene and iron bispentazole we analyzed the iron–ligand interactions between Fe^{2+} (t_{2g}, d^6) and two Cp^- or $cyclo-N_5^-$ ligands using the energy partitioning method, which is described in the Methods section.¹⁷ In this work we take the metal fragments $Fe(\eta^5-E_5)^+$ and the ligands $(\eta^5-E_5)^-$ for the analysis of the bonding interactions in the complexes. The advantage of the latter partitioning is that we can compare directly the

Table 4. Energy Decomposition Analysis of $Fe(E_5)_2$ Using the Fragments $Fe(E_5)^+$ and E_5^- (energy values in kcal/mol)

term	E = CH	E = N	E = P	E = As	E = Sb
ΔE_{int}	-237.6	-198.0	-199.5	-183.8	-165.1
ΔE_{Pauli}	172.4	149.7	190.2	221.6	220.8
ΔE_{elstat}^a	-238.5	-184.3	-207.3	-223.1	-205.1
	(58.2%)	(53.0%)	(53.2%)	(55.0%)	(53.1%)
ΔE_{orb}^a	-171.5	-163.4	-182.5	-182.3	-180.9
	(41.8%)	(47.0%)	(46.8%)	(45.0%)	(46.9%)
A_1^b	-25.0	-22.4	-28.1	-29.1	-35.7
	(14.6%)	(13.7%)	(15.4%)	(16.0%)	(19.7%)
A_2	0.0	0.0	0.0	0.0	0.0
E_1^b	-109.3	-106.1	-120.7	-123.7	-125.6
	(63.8%)	(65.0%)	(66.1%)	(67.8%)	(69.4%)
E_2^b	-37.1	-34.9	-33.7	-29.6	-19.6
	(21.6%)	(21.3%)	(18.5%)	(16.2%)	(10.8%)
ΔE_{prep}	2.8	13.1	28.0	23.3	46.3
$\Delta E (= -D_e)$	-234.8	-184.9	-171.5	-160.5	-118.8

^a The values in parentheses give the percentage contribution to the total attractive interactions. ^b The values in parentheses give the percentage contribution to the total orbital interactions.

iron–ligand bonding in $Fe(\eta^5-E_5)_2$ with $FeCp(\eta^5-E_5)$. The qualitative orbital correlation diagram for the interaction between Fe^{2+} and two $cyclo-E_5$ ligands is not very different from the diagram between $Fe(\eta^5-E_5)^+$ and $(\eta^5-E_5)^-$, which is shown in Figure 2.

The orbital diagram given in Figure 2 is adapted from similar diagrams which have been discussed in the literature.⁴⁵ According to the qualitative model, the most important orbital interactions take place (i) between the occupied e_1 (π) orbital of the ligand and the empty e_1 metal fragment orbital mainly via the d_{xz} and d_{yz} orbitals of Fe and (ii) between the empty e_2 (π) ligand orbital and the occupied e_2 metal fragment orbital mainly via the d_{xy} and $d_{x^2-y^2}$ orbitals of Fe. The interactions between the occupied a_1 orbitals of the ligand (lowest lying π orbital) and metal fragment (mainly via the d_z^2 Fe orbital) contribute to the bonding only by mixing in of the empty s and p_z orbitals of Fe. We will now discuss the results of the energy analysis in order to estimate quantitatively the strength of the orbital interactions with respect to each other and with respect to electrostatic attraction, which is not considered in the orbital correlation model.

It should be pointed out that the orbital correlation diagram shown in Figure 2, which presents the bonding in $Fe(\eta^5-E_5)_2$ in terms of interactions between $Fe(\eta^5-E_5)^+$ and $cyclo-E_5^-$, must not be confused with the actual driving force for the metal–ligand bonding. The dissociation products of the complex are neutral species, and a physically more realistic interpretation of the chemical bond would use the neutral radicals $Fe(\eta^5-E_5)$ and $cyclo-E_5$ as interacting fragments. The reason the charged closed-shell species are employed in the discussion of the chemical bonding is the conceptual simplicity that is given by this model. The neutral compound $cyclo-E_5$ with D_{5h} symmetry has a degenerate e_1 orbital that is occupied by three electrons, and thus, it is subject to Jahn–Teller distortion. The D_{5h} symmetry of the ligand comes from the bonding interactions with the metal, which leads to the occupation of the e_1 ligand orbital. It is important to recognize that this is the result but not the original driving force of the bonding interaction. It is conceptually much easier, however, to discuss the bonding between the charged closed-shell bonding frag-

Table 5. Energy Decomposition Analysis of FeCp(E_5) Using the Fragments FeCp $^+$ + E_5^- and Fe E_5^+ + Cp $^-$ (energy values given in kcal/mol)

term	FeCp $^+$ + E_5^-				Fe E_5^+ + Cp $^-$			
	E = N	E = P	E = As	E = Sb	E = N	E = P	E = As	E = Sb
ΔE_{int}	-164.5	-214.7	-202.3	-186.3	-298.6	-232.3	-228.1	-223.1
ΔE_{Pauli}	151.1	195.3	152.0	128.3	179.5	222.0	241.4	267.8
$\Delta E_{\text{elstat}}^a$	-177.2	-223.3	-196.6	-165.2	-257.8	-255.7	-265.3	-278.3
	(56.1%)	(54.5%)	(55.5%)	(52.5%)	(53.9%)	(56.3%)	(56.5%)	(56.7%)
ΔE_{orb}^a	-138.5	-186.7	-157.7	-149.3	-220.3	-198.6	-204.1	-212.6
	(43.9%)	(45.5%)	(44.5%)	(47.5%)	(46.1%)	(43.7%)	(43.5%)	(43.3%)
A_1^b	-18.9	-25.3	-23.6	-32.6	-28.9	-30.4	-33.0	-35.3
	(13.7%)	(13.6%)	(15.0%)	(21.8%)	(13.1%)	(15.3%)	(16.2%)	(16.6%)
A_2	0.0	0.0	0.0	0.0	0.0	0.0	0.0	0.0
E_1^b	-72.5	-98.4	-89.2	-88.8	-159.2	-144.9	-144.6	-150.2
	(52.3%)	(52.7%)	(56.5%)	(59.5%)	(72.3%)	(73.0%)	(70.8%)	(70.6%)
E_2^b	-47.1	-63.0	-45.0	-27.9	-32.2	-23.3	-26.5	-27.2
	(34.0%)	(33.7%)	(28.5%)	(18.7%)	(14.6%)	(11.7%)	(13.0%)	(12.8%)
ΔE_{prep}	6.2	5.3	4.4	4.1	9.9	11.9	14.5	32.5
$\Delta E (= -D_e)$	-158.3	-209.4	-197.9	-182.2	-288.7	-220.4	-213.6	-190.6

^a The values in parentheses give the percentage contribution to the total attractive interactions. ^b The values in parentheses give the percentage contribution to the total orbital interactions.

ments than between the neutral open-shell species. The calculated NBO charge distribution in the molecules gives the following values for the iron atom in Fe(η^5 - E_5) $_2$: +0.20 (E = CH), +0.65 (E = N), -0.05 (E = P), -0.63 (E = As), -0.13 (E = Sb). The partial charges at Fe in FeCp(η^5 - E_5) are +0.42 (E = N), -0.05 (E = P), -0.35 (E = As), and -0.03 (E = Sb).

Table 4 shows the results of the energy partitioning analysis of the homoleptic complexes Fe(η^5 - E_5) $_2$. Note that the instantaneous interaction energies ΔE_{int} of the nitrogen (-198.0 kcal/mol) and phosphorus (-199.5 kcal/mol) complexes are nearly the same. The larger bond dissociation energy of the former compound comes from the preparation energy ΔE_{prep} , which is smaller for Fe(η^5 -N $_5$) $_2$ (13.1 kcal/mol) than for Fe(η^5 -P $_5$) $_2$ (28.0 kcal/mol). The energy partitioning suggests that the bonding interactions between Fe(η^5 - E_5) $^+$ and *cyclo*- E_5^- are approximately half electrostatic and half covalent. The electrostatic contribution in ferrocene (58%) is a little higher than in the heterocyclic complexes (53–55%), but the differences are not very large. The covalent bonding in the latter species comes mainly from the e_1 orbitals, which contribute 65%–69% to the total orbital interaction term. There are also no significant differences among the different orbital contributions between ferrocene and the other sandwich complexes. The conclusion is that the nature of the bonding in the carbocyclic and heterocyclic Fe(η^5 - E_5) $_2$ complexes does not vary significantly from E = CH to E = Sb.

Table 5 gives the results of the energy analysis of the mixed complexes FeCp(η^5 - E_5). A comparison with the results of the homoleptic complexes shows nicely the differences between the metal–ligand interactions in the compounds. For example, the ΔE_{int} values of the interactions between the heterocyclic ligands *cyclo*- E_5^- and Fe(η^5 - E_5) $^+$ (Table 4) and between *cyclo*- E_5^- and FeCp $^+$ (Table 5) reveal that the nitrogen ring in the latter species is less strongly attracted than in the former compound, while the heavier heterocycles *cyclo*- E_5^- (E = P, As, Sb) in FeCp(η^5 - E_5) are more strongly attracted than in Fe(η^5 - E_5) $_2$. This means that the Cp ligand in FeCp(η^5 -N $_5$) weakens the bonding between *cyclo*-N $_5^-$ and FeCp $^+$ compared with Fe(η^5 -N $_5$) $_2$. Table 5 shows also that the nitrogen ring in FeCp(η^5 -N $_5$) strengthens the bonding between the Cp $^-$ ligand and

Fe(η^5 -N $_5$) $^+$ relative to FeCp $_2$. The smaller FeCp $^+$ -(η^5 -N $_5$) $^-$ interactions compared with Fe(η^5 -N $_5$) $^+$ -(η^5 -N $_5$) $^-$ can be explained with the weaker orbital attraction in the former compound which comes from the lower e_1 contribution (-72.5 kcal/mol) than in the latter molecule (-106.1 kcal/mol). This is because the donation from the occupied e_1 orbital of *cyclo*-N $_5^-$ into the empty e_1 orbital of the metal fragment Fe(η^5 - E_5) $^+$ (Figure 2) is weaker for E = CH than for E = N since nitrogen is more electronegative than CH. This is an example of how the qualitative bonding model shown in Figure 2 can be supported by a quantitative analysis which gives reasonable numbers for the pertaining entities.

The data in Table 5 show that there are no major changes in the relative contributions of the energy components in the mixed complexes compared with the homoleptic molecules. The bonding between FeCp $^+$ and *cyclo*- E_5^- and between Fe(η^5 - E_5) $^+$ and Cp $^-$ remains slightly more electrostatic than covalent. The e_1 contributions to the orbital interactions become smaller when the former interactions are considered, and they become stronger in the latter interactions. This reflects nicely the changes in the electronegativities.

5. Summary and Conclusion

The results of this work can be summarized as follows.

The homoleptic and heteroleptic sandwich complexes Fe(η^5 - E_5) $_2$ and FeCp(η^5 - E_5) are predicted to be energy minima on the potential energy surfaces. The strongest bonded homoleptic complex with a heterocyclic ligand *cyclo*- E_5 is Fe(η^5 -P $_5$) $_2$. The bond dissociation energy yielding the Fe atom and two *cyclo*-P $_5$ ligands (D_0 = 128.3 kcal/mol) is nearly the same as for ferrocene (D_0 = 131.3 kcal/mol). The nitrogen, arsenic, and antimony analogues of Fe(η^5 - E_5) $_2$ have significantly weaker metal–ligand bonds, which, however, should still be strong enough to make them isolable under appropriate conditions. The calculated heats of formation show also that the phosphorus complex is the most stable species of the heterocyclic Fe(η^5 - E_5) $_2$ series. The Fe-(η^5 - E_5) bonding in the mixed sandwich complexes FeCp(η^5 - E_5) is much stronger compared with the homoleptic molecules. The heterocyclic ligands *cyclo*- E_5 in the mixed complexes

$\text{FeCp}(\eta^5\text{-E}_5)$ bind as strongly or in case of phosphorus even stronger than one Cp ligand does in FeCp_2 except for $\text{E} = \text{Sb}$. The metal fragments $\text{Fe}(\eta^5\text{-E}_5)^+$ have a pyramidal geometry except for $\text{E} = \text{Sb}$. The cation $\text{Fe}(\eta^5\text{-Sb}_5)^+$ is predicted to be a planar ion that has D_{5h} symmetry.

The energy partitioning shows that the binding interactions between the closed-shell *cyclo-E*₅⁻ ligand and the $\text{Fe}(\eta^5\text{-E}_5)^+$ fragment do not change very much for the different ligand atoms E in the homoleptic and heteroleptic complexes. The bonding comes from 53%–58% electrostatic attraction, while 42%–47% come from

covalent interactions. The latter contribution comes mainly from the donation of the occupied e_1 (π) orbital of the ligand into the empty orbital of the metal fragment.

Acknowledgment. This work was supported by the Deutsche Forschungsgemeinschaft and by the Fonds der Chemischen Industrie. Excellent service by the Hochschulrechenzentrum of the Philipps-Universität Marburg is gratefully acknowledged. Additional computer time was provided by the HLRS Stuttgart.

OM020397A